

Supporting Information

Scission of 2D Inorganic Nanosheets via Physical Adsorption on a Nonflat Surface

Nobuyuki Sakai, Masahiko Suzuki, and Takayoshi Sasaki*

This file includes six supplementary figures and one supplementary table.

Figure S1. Synthesis procedures of $\text{Ti}_{0.87}\text{O}_2^{0.52-}$ nanosheets.

Figure S2. Density of Ti–O bonds across vertical lattice plane of the $\text{Ti}_{0.87}\text{O}_2^{0.52-}$ nanosheet.

Figure S3. SEM images of $\text{Ca}_2\text{Nb}_3\text{O}_{10}^-$ nanosheets on a bumpy surface.

Figure S4. LEEM/LEED for $\text{Ti}_{0.87}\text{O}_2^{0.52-}$ nanosheets on an unpolished bumpy ITO surface.

Figure S5. Schematic illustration of the reciprocal space and corresponding LEED patterns.

Figure S6. SEM images of $\text{Ti}_{0.87}\text{O}_2^{0.52-}$ nanosheets electrostatically adsorbed on ITO surfaces.

Table S1. Calculated threshold for scission of various 2D nanosheets.

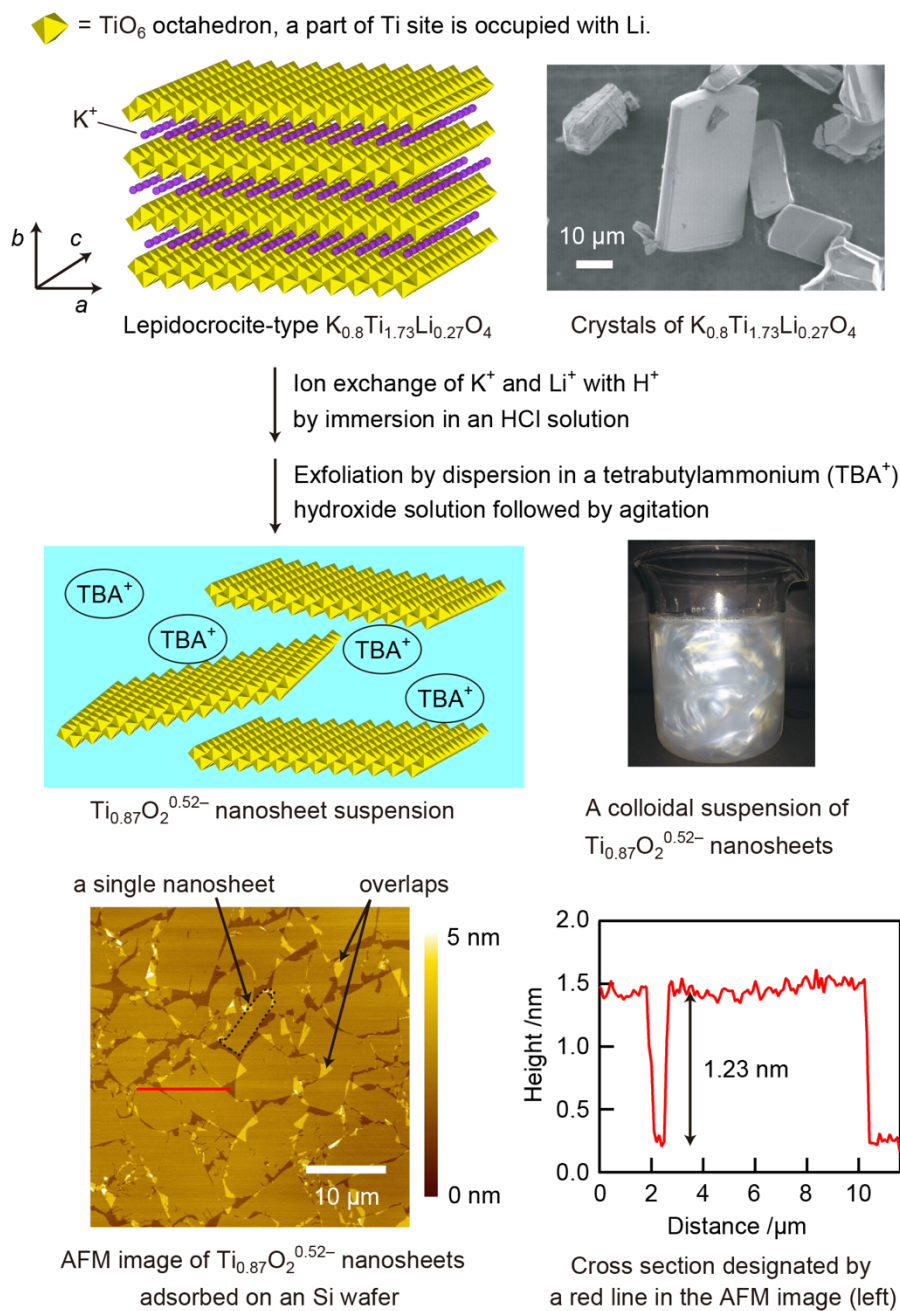


Figure S1. Synthesis procedures of $\text{Ti}_{0.87}\text{O}_2^{0.52-}$ nanosheets by soft-chemical processes through exfoliation of the layered lepidocrocite-type titanate into elementary layers. The negative charges of the nanosheets are balanced by the adsorbed protons and TBA^+ ions. The nanosheets are obtained as a colloidal suspension and can be adsorbed on a substrate via solution processes. The thickness of the nanosheets is ~ 1.2 nm.

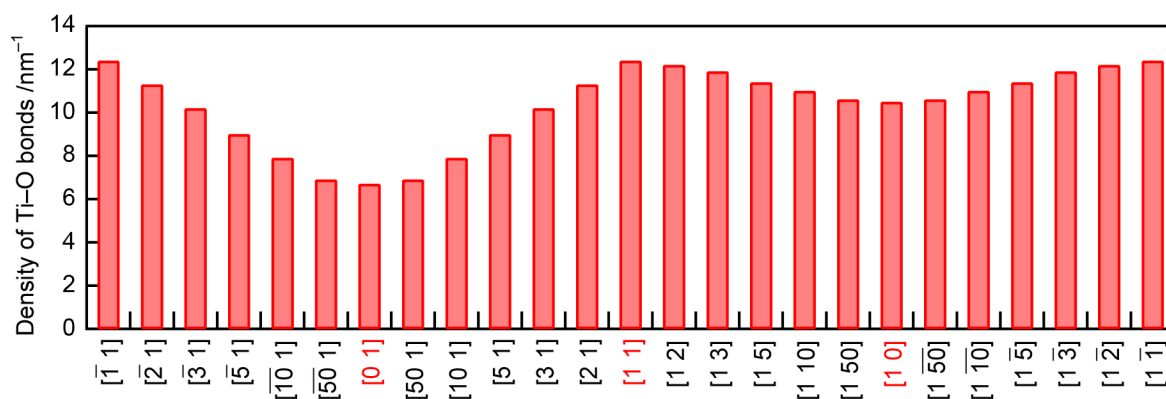


Figure S2. Density of Ti–O bonds across a lattice plane perpendicular to the lateral direction of the $\text{Ti}_{0.87}\text{O}_2^{0.52-}$ nanosheet plotted against the corresponding axis.

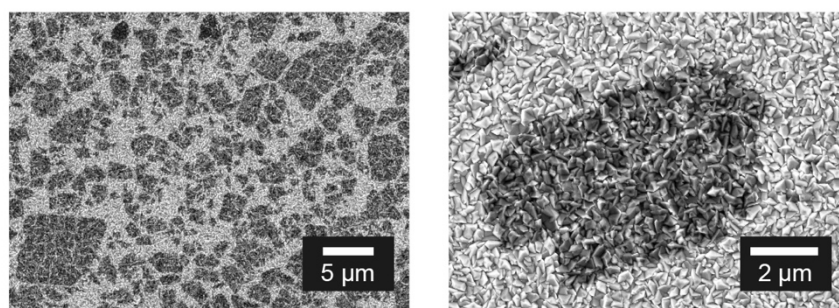


Figure S3. SEM images of $\text{Ca}_2\text{Nb}_3\text{O}_{10}^-$ nanosheets spin-coated on a fluorine-doped tin oxide (FTO) substrate with a bumpy surface ($R_a = 27 \text{ nm}$, $\theta = \tan^{-1}(0.4)$). The preparation method of $\text{Ca}_2\text{Nb}_3\text{O}_{10}^-$ nanosheets dispersed in DMSO can be found elsewhere.^[41]

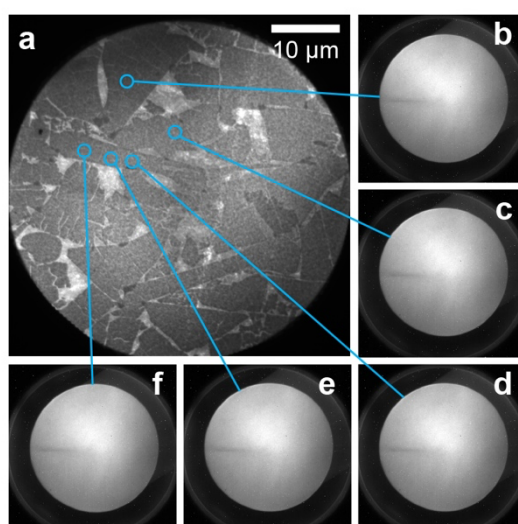


Figure S4. a) LEEM image of $\text{Ti}_{0.87}\text{O}_2^{0.52-}$ nanosheets on an unpolished bumpy ITO surface. b–f) LEED patterns acquired at an acceleration energy of 30 eV for each area designated by a blue circle (the diameter $\sim 0.4 \mu\text{m}$).

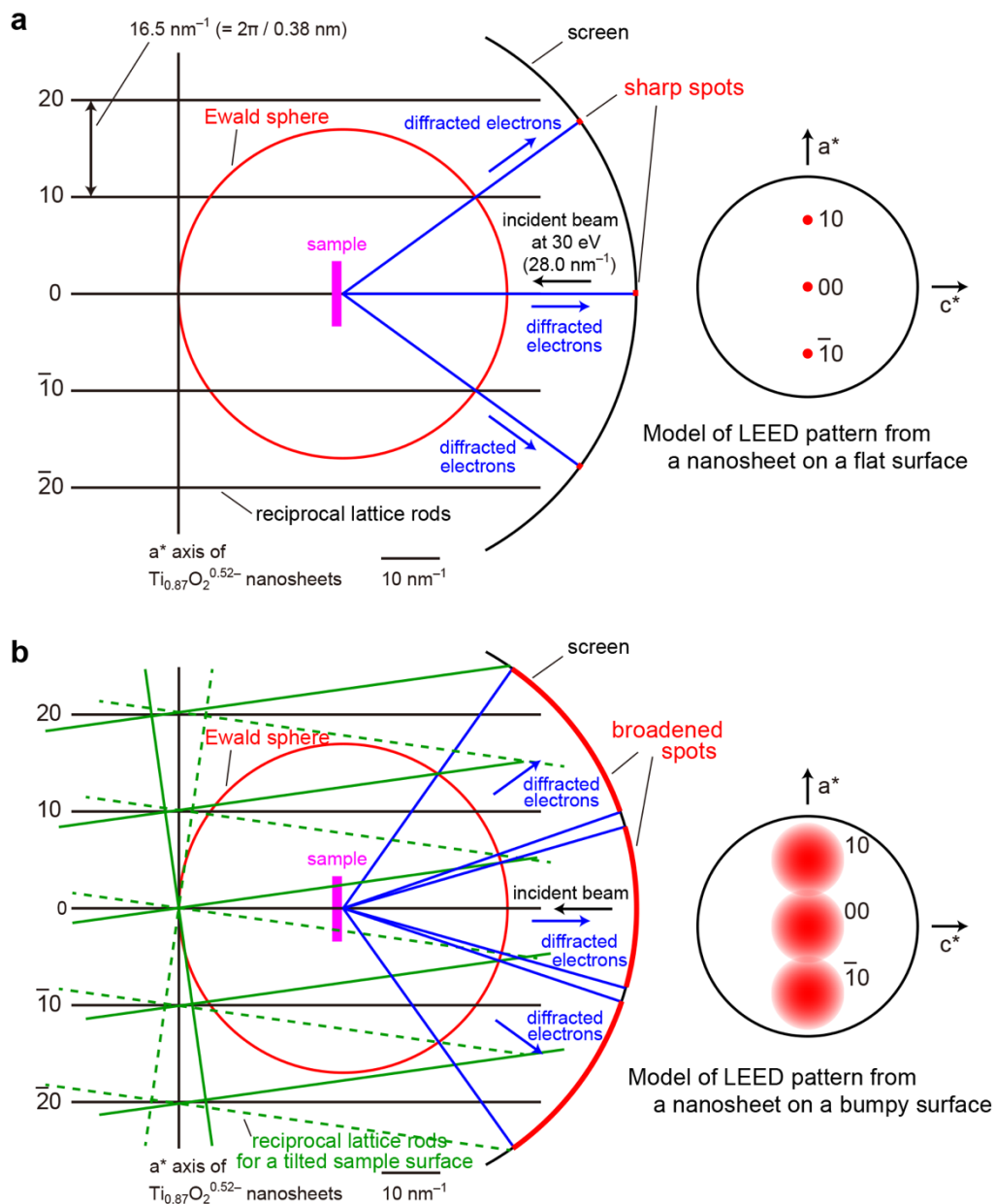


Figure S5. Schematic illustration of the reciprocal space of the sample on flat and bumpy surfaces and corresponding diffraction patterns. a) When the sample surface is flat and the electron beam is irradiated normal to the surface, sharp spots can be observed. b) When the sample surface is bumpy, the spots are significantly broadened and eventually become coalescent to yield very wide diffraction feature because the crystal plane of the sample is tilted and its angle varies within a certain range.

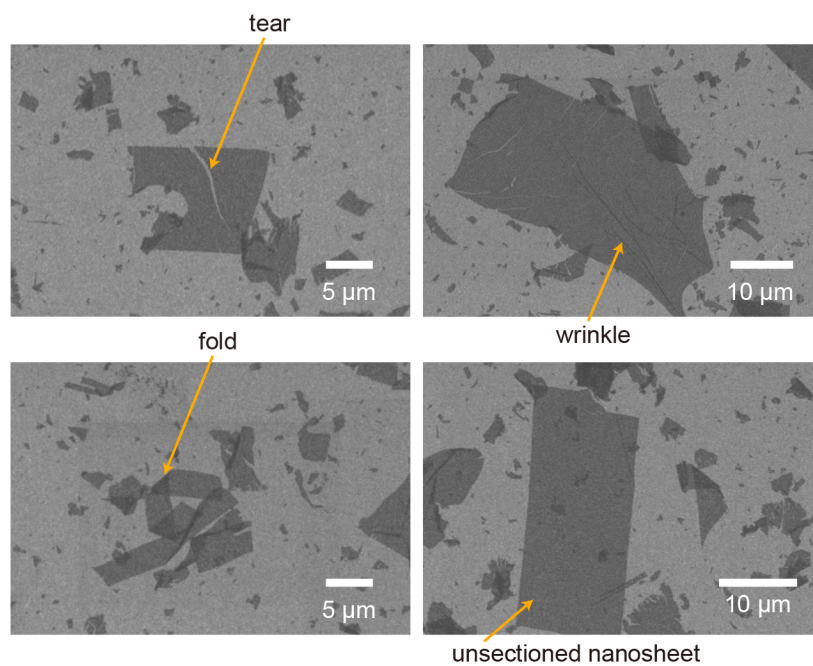


Figure S6. SEM images of $\text{Ti}_{0.87}\text{O}_2^{0.52-}$ nanosheets on a bumpy ITO surface. The nanosheets were electrostatically adsorbed on the ITO surface pre-coated with cationic polymers.

Table S1. Calculated threshold of the lateral size for scission of various 2D nanosheets along the [10]-axis direction on the assumption that the nanosheets dispersed in DMSO are spin-coated onto the bumpy ITO surface.

	Graphene	MoS ₂ nanosheet	Ca ₂ Nb ₃ O ₁₀ ⁻ nanosheet
Unit cell	2D Hexagonal	2D Hexagonal	2D Square
Lattice constant	$a = 0.246 \text{ nm}$ ^[S1]	$a = 0.316 \text{ nm}$ ^[S2]	$a = 0.390 \text{ nm}$ ^[S3]
Binding energy	848 kJ/mol (C–C (sp ²)) ^[S4]	433 kJ/mol (Mo–S) ^[S5]	770 kJ/mol (Nb–O) ^[S6]
Number of bonds within the unit cell	1	2	3
Surface free energy	53.0 mJ/m ² ^[S7]	54.5 mJ/m ² ^[S8]	73.7 mJ/m ² ^[S9]
Threshold of the lateral size for scission	600 nm	470 nm	760 nm

[S1] C. Tan, X. Cao, X.-J. Wu, Q. He, J. Yang, X. Zhang, J. Chen, W. Zhao, S. Han, G.-H. Nam, M. Sindoro, H. Zhang, *Chem. Rev.* **2017**, *117*, 6225.

[S2] X. Huang, Z. Zeng, H. Zhang, *Chem. Soc. Rev.* **2013**, *42*, 1934.

[S3] K. Akatsuka, G. Takanashi, Y. Ebina, M. Haga, T. Sasaki, *J. Phys. Chem. C* **2012**, *116*, 12426.

[S4] M. C. Schabel, J. L. Martins, *Phys. Rev. B* **1992**, *46*, 7185.

[S5] X. Liu, D. Cao, T. Yang, H. Li, H. Ge, M. Ramos, Q. Peng, A. K. Dearden, Z. Cao, Y. Yang, Y.-W. Li, X.-D. Wen, *RSC Adv.* **2017**, *7*, 9513.

[S6] Y.-R. Luo, *Comprehensive Handbook of Chemical Bond Energies*, CRC Press, **2007**.

[S7] A. Kozbial, Z. Li, C. Conaway, R. McGinley, S. Dhingra, V. Vahdat, F. Zhou, B. D'Urso, H. Liu, L. Li, *Langmuir* **2014**, *30*, 8598.

[S8] A. Kozbial, X. Gong, H. Liu, L. Li, *Langmuir* **2015**, *31*, 8429.

[S9] Based on the contact angle measurements: 0.3° for water and 36.2° for methylene iodide.